

Supplementary Materials

Table S1. Change rates of the $\delta^{13}\text{C}_{\text{cor}}$, $\delta^{18}\text{O}$ and intrinsic water-use efficiency ($i\text{WUE}$) series in the drought strengthened period ($D_{\text{s}+}$, 1986–1999) or in the drought weakened period ($D_{\text{s}-}$, 2000–2017) calculated using simple piecewise regression based on the data of *Pinus tabuliformis* and *Sophora viciifolia*.

	Period	$\delta^{13}\text{C}_{\text{cor}} (\text{\textperthousand yr}^{-1})$	$\delta^{18}\text{O} (\text{\textperthousand yr}^{-1})$	$i\text{WUE} (\mu\text{mol mol}^{-1} \text{yr}^{-1})$
<i>P. tabuliformis</i>	$D_{\text{s}+}$	0.373***	-0.002	4.57***
	$D_{\text{s}-}$	-0.064	-0.042	0.47
<i>S. viciifolia</i>	$D_{\text{s}+}$	0.367	0.460	4.64
	$D_{\text{s}-}$	0.004	-0.117*	1.28***

Significance levels are presented by * and ***: * $p < 0.05$; *** $p < 0.005$.

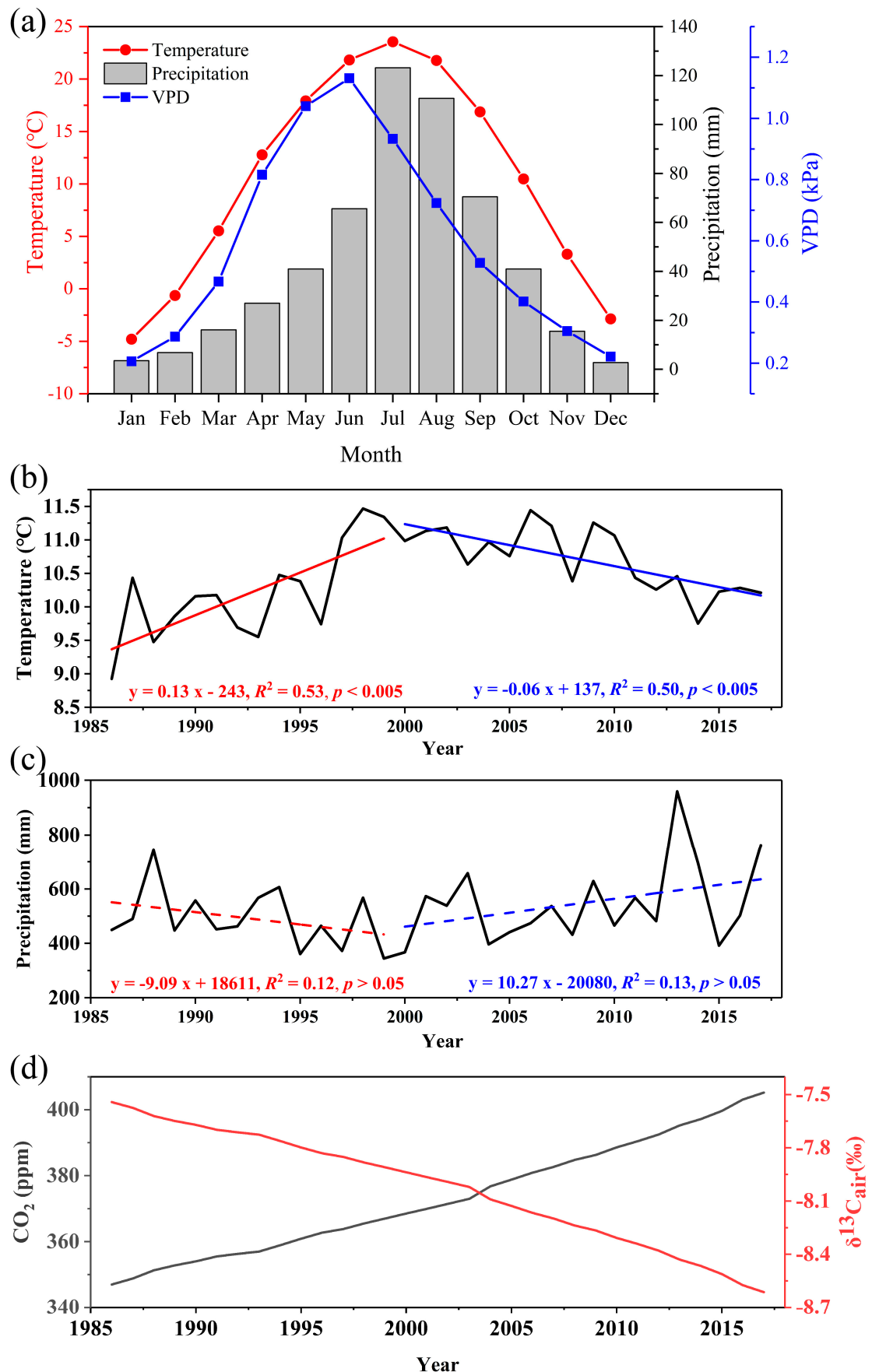


Figure S1. (a) The monthly mean temperature, precipitation and vapor-

pressure deficit (*VPD*) at the Yan'an meteorological station. Temporal variations of the annual (b) mean annual temperature, (c) total precipitation and (d) atmospheric carbon dioxide concentration (CO_2 , grey line) and atmospheric stable carbon isotope ratio ($\delta^{13}\text{C}_{\text{air}}$, red line) from 1986 to 2017. We divide the entire period into two sub-periods based on the change in drought trends that occurred in 2000. The trends and linear regression models for mean annual temperature and total precipitation in the two sub-periods are also provided. The solid and dashed lines represent significant and nonsignificant trends, respectively.

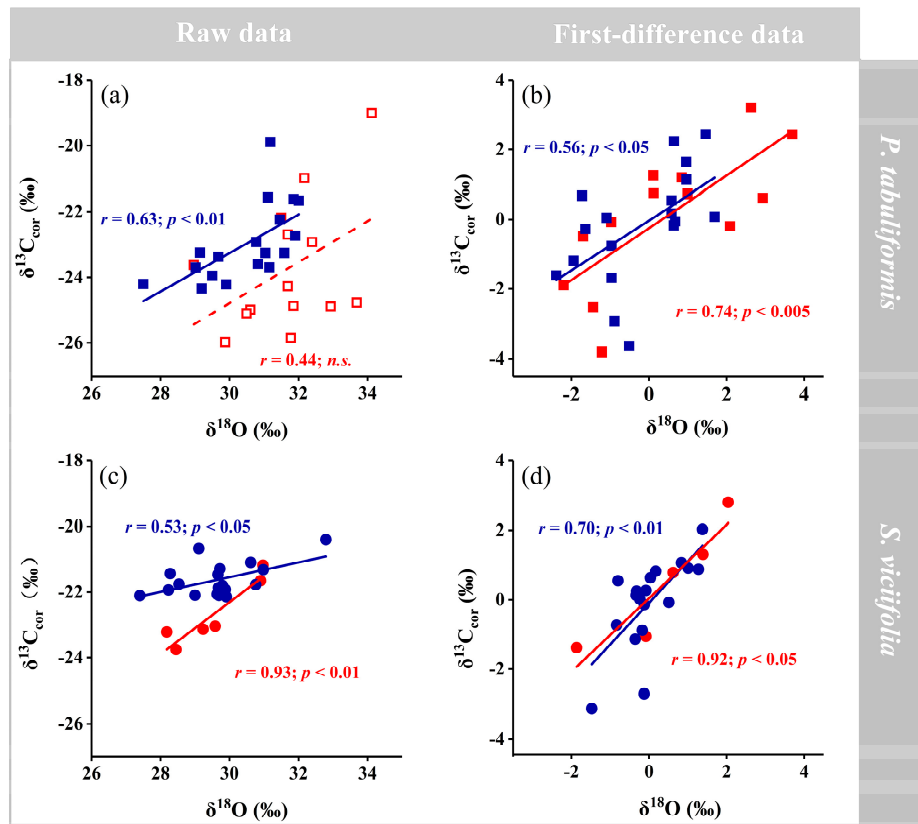


Figure S2. Scatter plots for the relationships between the tree-ring $\delta^{13}\text{C}_{\text{cor}}$ and $\delta^{18}\text{O}$ series during the period when drought stress strengthened (light red) and the period when drought stress weakened (dark blue) for (a, b) *Pinus tabuliformis* and (c, d) *Sophora viciifolia*: (a, c) raw data, (b, d) the first-difference data. The Pearson correlation coefficients (r) for the two subperiods is provided. The solid and dashed lines represent significant and nonsignificant trends, respectively. *n.s.*: non-significant ($p > 0.05$).

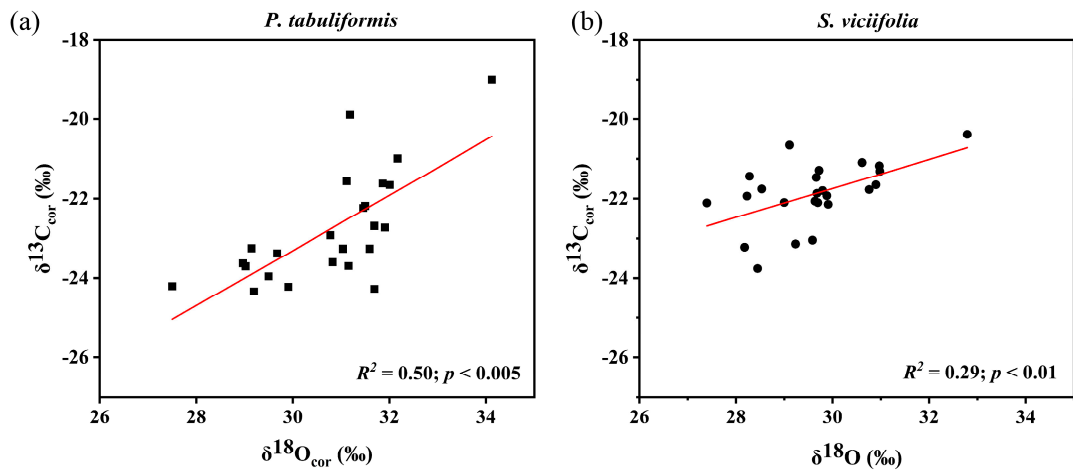


Figure S3. Scatter plots for the relationships between the tree-ring $\delta^{13}\text{C}_{\text{cor}}$ and $\delta^{18}\text{O}$ series during the common period from 1994 to 2017 for (a) *Pinus tabuliformis* and (b) *Sophora viciifolia* in the raw data. The coefficient of determination (R^2) is provided.

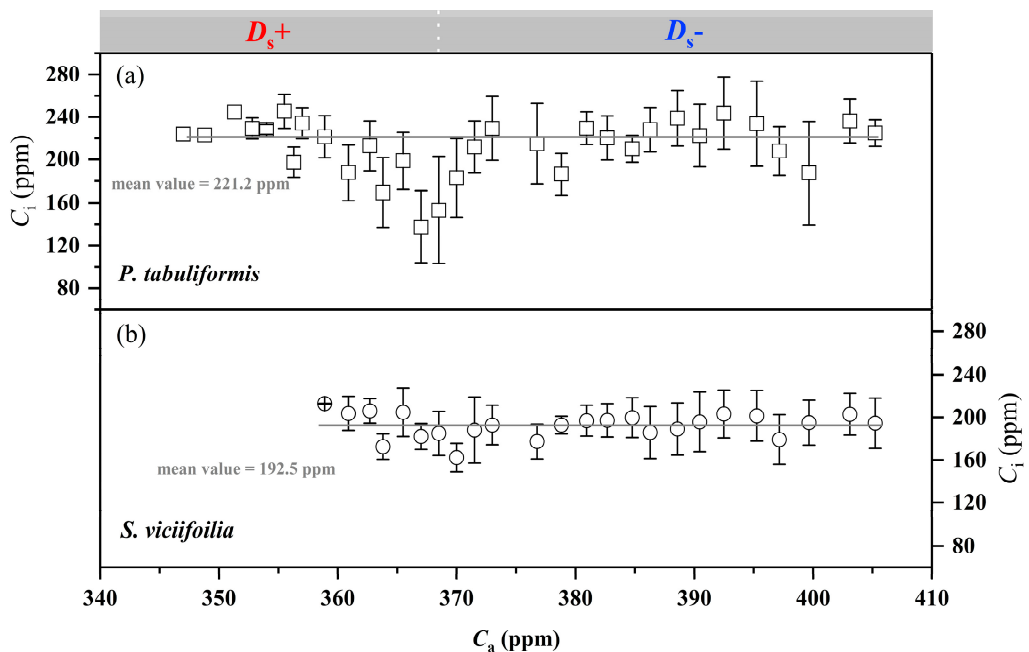


Figure S4. The trends of intercellular CO₂ concentration (C_i) based on tree-ring $\delta^{13}\text{C}_{\text{plant}}$ of *Pinus tabuliformis* (a) and *Sophora viciifolia* (b) as atmospheric CO₂ concentration (C_a) rises. The grey straight lines indicate the mean value of intercellular CO₂ concentration (C_i). Error bars are 1 standard deviation (SD). D_s+ = the period when drought stress strengthened; D_s- = the period when drought stress weakened.